Scripta Materialia 157 (2018) 44–48

Contents lists available at ScienceDirect

Scripta Materialia

journal homepage: www.elsevier.com/locate/scriptamat

Regular article

Rapid measurement of volumetric texture using resonant ultrasound spectroscopy

Bo Lan[a,*], Michael A. Carpenter[b], Weimin Gan[c], Michael Hofmann[d], Fionn P.E. Dunne[e], Michael J.S. Lowe[a]

[a]Department of Mechanical Engineering, Imperial College London, UK
[b]Department of Earth Sciences, University of Cambridge, UK
[c]German Engineering Materials Science Centre at MLZ, Helmholtz-Centre Geesthacht, Germany
[d]Heinz Maier-Leibnitz Zentrum (MLZ), Technische Universität München, Germany
[e]Department of Materials, Imperial College London, UK

ARTICLE INFO

Article history:
Received 19 May 2018
Received in revised form 20 July 2018
Accepted 21 July 2018
Available online 1 August 2018

Keywords:
Crystallographic texture
Resonant ultrasound spectroscopy
Non-destructive evaluation

ABSTRACT

This paper presents a non-destructive evaluation method of volumetric texture using resonant ultrasound spectroscopy (RUS). It is based on a general theoretical platform that links the directional wave speeds of a polycrystalline aggregate to its texture through a simple convolution relationship, and RUS is employed to obtain the speeds by measuring the elastic constants, where well-established experimental and post-processing procedures are followed. Important lower-truncation-order textures of representative hexagonal and cubic metal samples with orthorhombic sample symmetries are extracted, and are validated against independent immersion ultrasound and neutron tests. The successful deployment of RUS indicates broader applications of the general methodology.

Crystallographic texture refers to the preferred orientation distributions in polycrystalline aggregates that are often formed during the thermal-mechanical processing procedures [1]. It dominates macroscopic physical properties [1,2], such as strength, thermal expansion and fatigue lives, hence is of great importance for various industrial applications. Unfortunately, despite texture being a volumetric concept, existing lab-based techniques (e.g. X-ray [3], electron back-scattered diffraction [4] and surface acoustic wave-based [5] methods) are confined to surface or near-surface inspections, and the bulk texture can only be obtained at large-scale neutron or X-ray synchrotron facilities with limited access [6].

Ultrasound presents an attractive option for non-destructive evaluation of volumetric texture, given its high penetration power and wide availability. Early developments in this direction (e.g. [7-9]) mainly focussed on guided (not bulk) waves in rolled plates, but the inversion involved highly cumbersome iterative least-square fitting processes, which could also lead to inaccurate and non-unique solutions. A general theoretical platform proposed by the authors [10, 11] gave a viable solution to obtaining texture using direction-dependent bulk compressional wave speeds, where high accuracy and uniqueness could be simultaneously achieved via a simple deconvolution process. It has been comprehensively validated against neutron diffraction experimentally using a conventional immersion ultrasonic system [12]. However, that particular setup requires relatively large samples to be immersed in water for sophisticated directional speed measurements. Since the theories are general and independent of the specific experimental technique, resonant ultrasound spectroscopy (RUS) provides an alternative way to extracting texture while circumventing those limitations.

RUS is an established technique for measuring elastic constants, and has been attempted for texture inversions before [13,14]. Instead of directly fitting the elastic constants, those authors explicitly expressed them in terms of orientation distribution coefficients (ODCs) through complicated homogenisation methods (most commonly the Voigt average), and iteratively fitted the ODCs using a customised protocol. Here we show that by introducing the convolution platform, the extraction of texture can be done after the elastic constants are obtained, so that the standard RUS experimental and data post-processing procedures can remain untouched, and one only needs to solve the classic wave equation to obtain the required speeds for texture, all achieved directly without iterations. Thus this approach greatly reduces the complexity of the inversion process,

* Corresponding author.
E-mail address: bo.lan@imperial.ac.uk (B. Lan).

https://doi.org/10.1016/j.scriptamat.2018.07.029

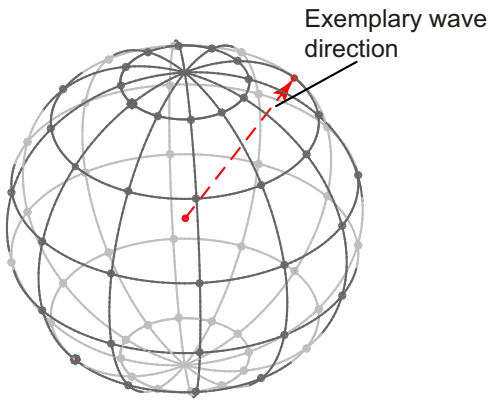

Fig. 1. 6×12 discrete directions needed for numerical integration of V_{lm} when $N = 6$ [12]. Note that the reciprocity of wave speeds reduces the number by half.

and is in a better position to take advantage of the latest technical advancement on RUS (e.g. on laser excitation [14]).

The theoretical basis of the convolution method is that in a directionally homogeneous polycrystal, the three-dimensional wave speed variations can be approximated, to excellent precision, by a spherical convolution between single crystal wave speeds and texture [10, 11]:

$$V_{lm} = \sum_{n=-l}^{l} W_{lmn} K_{ln} \tag{1}$$

where V_{lm} and K_{ln} are the series expansion coefficients of the poly- and single crystal wave speeds with respect to spherical harmonics $Y_{lm}(\theta_i, \phi_j)$, while W_{lmn} are the coefficients of the orientation distribution function (ODF) $w(\psi, \theta, \phi)$ expanded on Wigner-D functions. In the special case of hexagonal materials, where only the c-axis texture affects wave speeds (due to the elastic transverse isotropy of the single crystals), the convolution relationship can be further simplified as [10]:

$$V_{lm} = W_{lm0} K_{l0}. \tag{2}$$

The three variables in Eqs. (1) and (2) are linked by simple, pointwise multiplications of expansion coefficients that can be deployed in both forward and inverse studies. The correspondences between coefficients are unique, and applying the equations in either direction does not involve any fitting [10]. The limitation of this technique, however, is that only the ODF coefficients up to the 4th order can be reliably retrieved from elastic waves (or elasticity in general). This is because the 4th-rank elastic tensor - which intrinsically possesses 4-fold rotation symmetry - has only minimal physical coupling with the higher-order expansion bases of higher symmetries [11,15].

Of the variables, the single crystal speeds can be calculated from available elastic constants, so the key to inversely retrieving texture (as ODF coefficients W_{lmn}) is to obtain V_{lm}. This can be achieved via numerical integration of polycrystal velocities $v(\theta_i, \phi_j)$ in discrete directions [10]:

$$V_{lm} = \frac{\pi}{N} \sum_{j=0}^{2N-1} \sum_{i=0}^{N-1} v(\theta_i, \phi_j) Y^*_{lm}(\theta_i, \phi_j) \omega_N(i) \tag{3}$$

This integration scheme prescribes the discrete directions corresponding to the Gaussian-Legendre quadrature, as shown in Fig. 1, which will be determined from elastic constants measured by RUS.

Industry-relevant metal samples of hexagonal and cubic crystal symmetries are examined to demonstrate the texture inversion, including commercially pure titanium (CP Ti) and Ti-6Al-4 V (both hexagonal, though Ti-6Al-4 V contains ~10% of cubic beta-phase and is intended as a challenging case), which are used extensively in the aerospace industry; and 304 stainless steel (cubic) found in a wide range of civil engineering applications.

The samples are all cut from rolled plates or sheets along the principal sample axes (hence all have orthorhombic sample symmetry), into rectangular parallelepipeds of ~3 × 4 × 5mm^3. The RUS

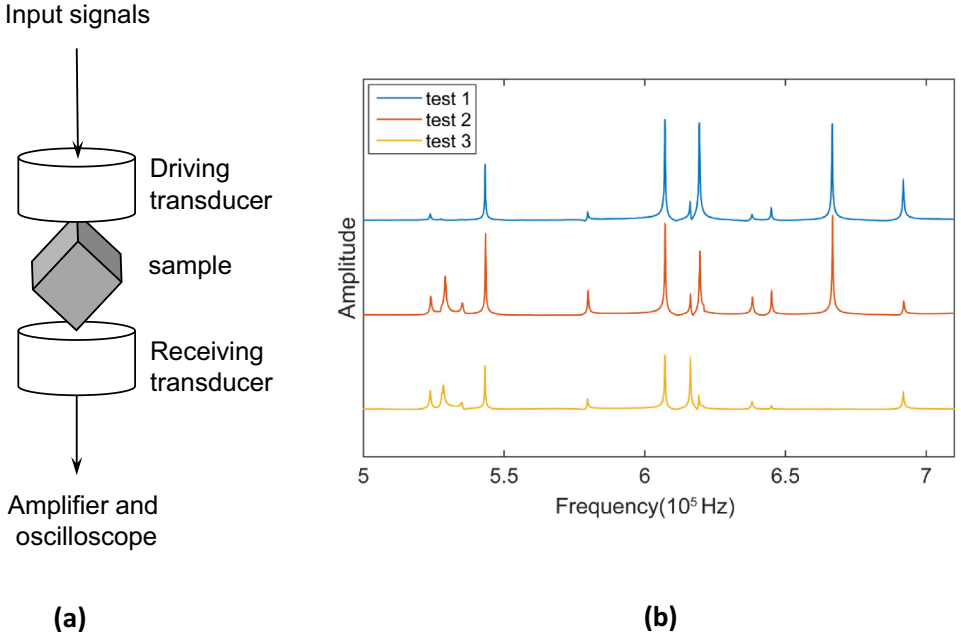

Fig. 2. (a) Schematics of the RUS setup; (b) The frequency-amplitude spectra obtained in different mounting positions (shown by different colours with artificial vertical shifts) help identify all natural vibrational modes.
Source: (Source: This figure is reproduced from [18].)

Table 1
Polycrystal density and elastic constants of the experimental hexagonal and cubic materials measured by RUS (units: ρ: g•cm^{-3}, elastic constants: GPa).

	ρ	c_{11}	c_{22}	c_{33}	c_{23}	c_{13}	c_{12}	c_{44}	c_{55}	c_{66}	Residual (%)
CP Ti	4.42	160.9	160.8	170.4	73.2	70.8	84.7	46.9	44.4	38.2	0.23
Ti-6Al-4 V	4.37	171.9	176.3	165.9	78.5	84.0	76.9	45.2	42.3	47.9	0.13
304SS	7.81	259.0	269.1	261.3	101.6	112.8	107.0	70.8	81.4	74.5	0.13

measurements are performed on a standard platform manufactured by Dynamic Resonance System (DRS) at University of Cambridge, UK [16]. During the tests, the sample is held with minimum contact between two piezoelectric transducers, one of which excites mechanical vibrations into the sample while the other detects at the other end. As the input vibrational frequency is swept across the spectrum, those corresponding to the natural frequencies of the sample would cause much higher amplitudes on the receiving transducer, resulting in spikes on the frequency-amplitude plot; by recording the plots at multiple sample mounting positions, all resonant modes can be identified sequentially without missing any, as shown in Fig. 2.

It has been theoretically proved that the resonant frequencies satisfy both the wave equation and free surface boundary conditions [17], so the elastic constants can be inversely retrieved through an iterative process combining forward modelling of the natural modes for the given sample geometries using the Rayleigh-Ritz method, and minimisation of the differences between modelled and tested values using algorithms such as the Levenberg-Marquardt [17]. A figure of merit F is defined to aid the minimisation process to a designated value:

$$F = \sum_{i=1}^{N} w_i (f_i - g_i)^2, \tag{4}$$

where f and g are the modelled and experimental frequencies, and the weighting factor w_i reflects the confidence of the N number of frequencies. As many as ~65 modes are used to achieve optimal accuracy for each of our samples, for which 9 elastic constants are unknown (the other constants are negligibly small [18] due to orthorhombic sample symmetry).

This elastic constants inversion process is a well-established practice, and the standard open-source codes by Migliori and Sarrao [17] are employed to retrieve the elastic constants. The results are listed in Table 1 [18], and good fitting qualities are achieved, as indicated by the low levels (all $< 0.25\%$) of residuals (root-mean square errors).

Extracting texture from the determined elastic constants is now straightforward and no longer involves fitting: firstly, the longitudinal wave phase velocities $v(\theta_i, \phi_j)$ required in Eq. (3) are obtained as solutions to the well-known Christoffel determinant in the direction $\mathbf{n} = (\cos\phi_j sin\theta_i, \sin\phi_j sin\theta_i, \cos\theta_i)$:

$$|c_{ijkl} n_j n_k - \rho v^2 \delta_{il}| = 0 \tag{5}$$

where δ_{il} is the Kronecker delta; then the V_{lm} values can be used to either reconstruct the 3D wave speed variation surface, or be input to Eqs. (1) and (2) for texture inversion. Here both the speed surfaces and obtained textures are compared with those from immersion ultrasonic tests (directly measured using a conventional water-bath scanning system in [12]) to demonstrate the efficacy of the RUS technique.

The surfaces are constructed from V_{lm} values via spherical harmonic synthesis:

$$v(\theta, \phi) = \sum_{l=0}^{N} \sum_{m=-l}^{l} V_{lm} Y_{lm}(\theta, \phi) \tag{6}$$

which gives a smoothly varying surface covering all directions. The stereographic projections of such surfaces obtained by RUS and immersion tests are listed in Fig. 3. Generally good agreements are achieved between the two techniques, especially on the overall variation patterns. There are noticeable shifts (~50 m /s) in the average wave speed levels, which are probably caused by the (inevitable) experimental and fitting errors of the RUS elastic constants.

From a series expansion point of view (analogous to Fourier series in two dimensions), the average speed level is a constant in all directions, and is mainly reflected by the 0th-order harmonics coefficient; while the variations fluctuating with directions are dominated by the higher-order ones. When using Eqs. (1) and (2) for texture, the 0th order term V_{00} is discarded, since the ODF coefficient W_{000} is always =1 regardless of texture, and does not need to be recovered from wave speeds. As such, the shifts of average RUS speeds never

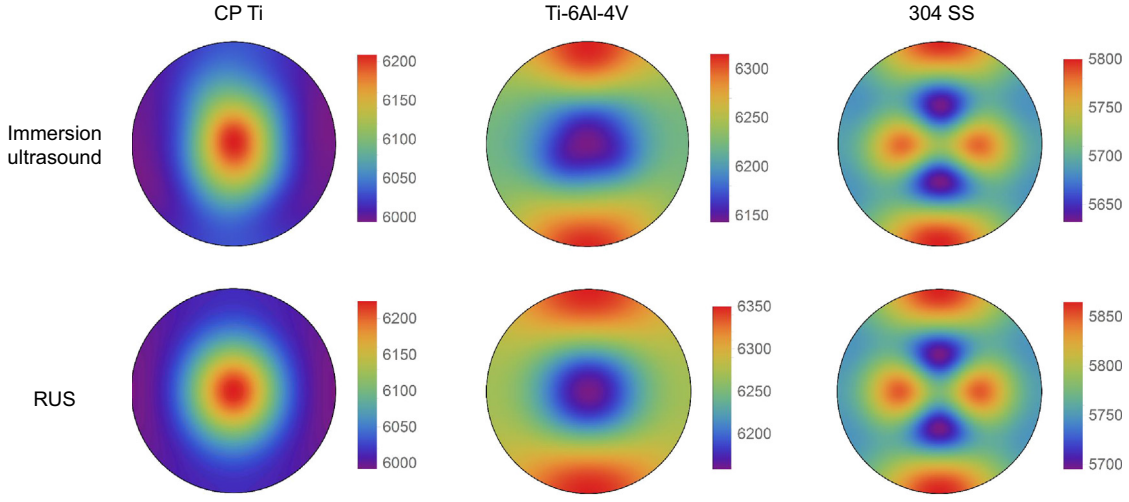

Fig. 3. Reconstructed wave speed surfaces from RUS elastic constants and direct immersion measurements.

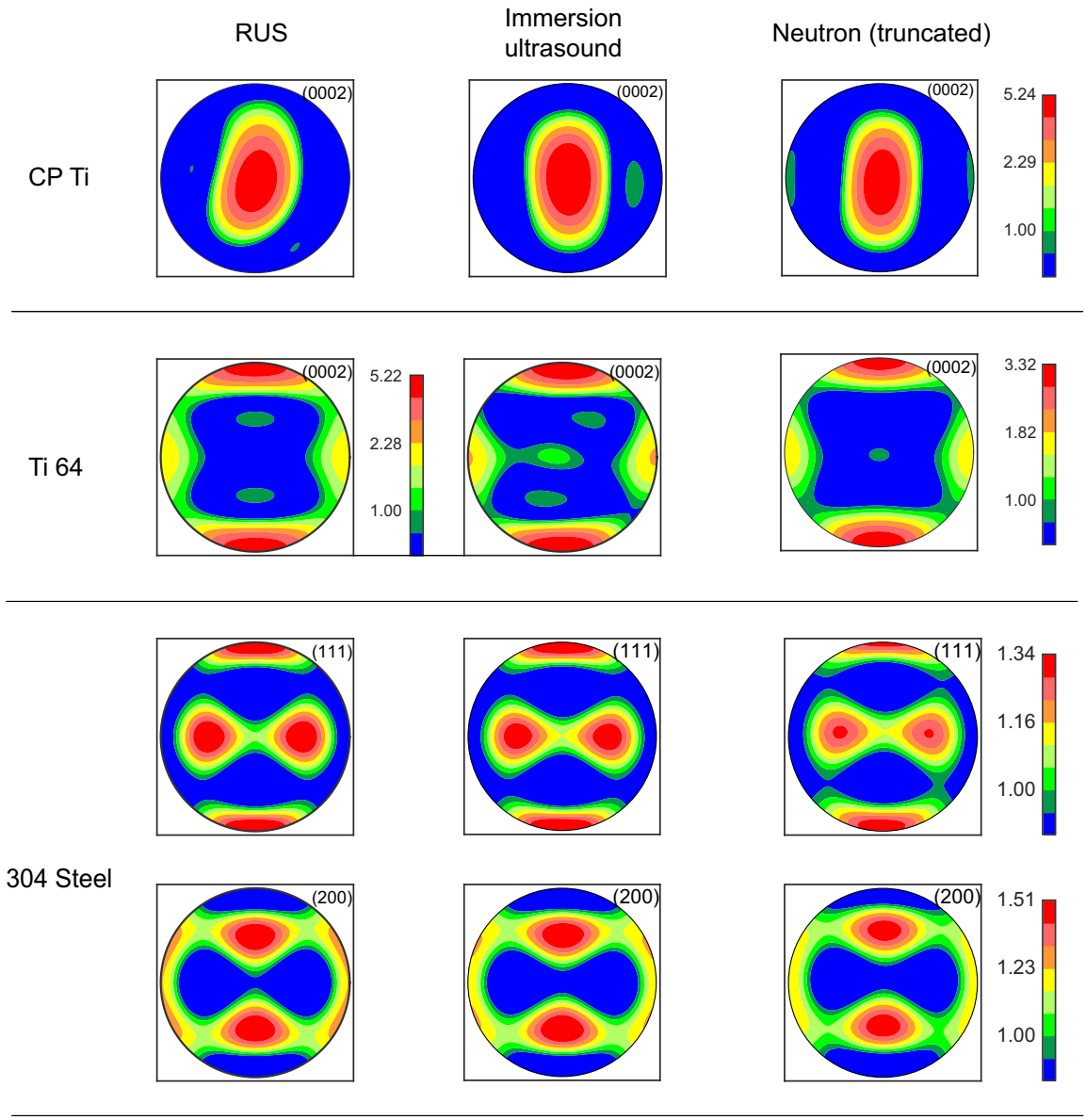

Fig. 4. Texture results (shown as pole figures) for the three samples, obtained from RUS, immersion ultrasound and neutron diffraction tests. Note that the neutron results are truncated to the 4th order spherical expansion for a direct comparison with the elastic methods.

enter the inversion process, and do not cause numerical errors to the texture results. For the 2nd- and 4th-order coefficients that do matter for the inversion, good qualitative (as manifested by the speed surfaces) and numerical accuracies are achieved, as demonstrated by the texture results below.

The textures inverted from the RUS measurements are shown in Fig. 4 as pole figures (stereographic projections of orientation distributions in 3D), in comparison with those obtained from directly measured speeds of the immersion tests. In addition, these samples have been examined by the golden standard of volumetric texture measurements that is neutron diffraction (performed at the monochromatic neutron facility Stress-Spec [19] at FRM II, MLZ, Germany, details in [12]), with the results truncated to the same 4th-order for a direct benchmark for the elastic methods. Their full forms may be found in [12].

It is evident that for all the samples, the RUS textures generally reproduce those from immersion tests well, in accordance with the good agreements between their wave speed patterns. These agreements are also extended to the neutron results, on both the overall distributions and numerical intensities. One exception is that the distribution pattern of CP Ti is slightly distorted or rotated (though the near basal texture is recognisable), which, again, is probably caused by experimental (e.g. sample cutting or mounting) and fitting errors. Another notable difference is the intensities of the Ti-6Al-4V sample between the elastic and neutron methods, which are not errors, but are caused by the different treatments of its beta phase: the elastic methods assume the alpha phase is responsible for the elastic anisotropy and the beta has random texture, while the neutron is unable to deconvolve the overlapping alpha(0001)-beta(002) peaks and assumes intensity is all from the alpha phase [12] - neither is perfectly accurate, but the agreements of the overall distribution pattern nonetheless demonstrate the robustness of the method. Therefore, it suffices to say that the RUS-based texture inversion has been successful for these representative samples.

The reader should be reminded that even though the results of both acoustic methods agree well with the truncated neutron in Fig. 4, the latter technique can easily obtain >20 orders of ODF coefficients and provide superior resolutions. However, for evaluations of ≤ 4th-rank tensor properties, such as thermal expansion (vital for Zr in nuclear industries), magnetism and elasticity etc., only the lower-order coefficients are involved, so that the acoustic methods achieve the same practical values as neutron, and their advantages of rapid and non-destructive measurements, and wide and cheap availability, are highlighted. One may also establish empirical links to connect the acoustic texture with the full ones if the latter are needed, by utilising the fact that the plastic deformation mechanisms causing texture could also result in interlocking coefficients for these crystal systems.

As a short summary of this study, the well-established RUS technique is used as an experimental means for the validation of a theoretical platform that enables the extraction of crystallographic texture information from compressional wave speeds. The standard RUS routine of measuring elastic constants is first conducted on representative metal samples, with the obtained results input to the wave equation to calculate the wave speeds, which are then input to the convolution model to extract the texture information. The end results are successfully compared against previously obtained textures from independent immersion ultrasonic [12] and neutron diffraction tests.

Since the RUS experiments follow the standard routine without changing any of its protocols, and the data are post-processed using existing open-source software, this study establishes the RUS as another easy-to-implement, accessible means to extract bulk texture information. The successful deployment of RUS for texture deconvolution also proves the generality of the underlying theoretical platform: it is arbitrarily scalable in both temporal and spatial dimensions, and is equally applicable to MHz ultrasound on 20 mm samples and kHz vibrations in <5 mm samples. It therefore gives hard evidence for broader application of the approach on engineering problems (e.g. to explore the shear wave propagation in textured polycrystals) and to geology (e.g. on interrogation of textures in planetary structures using seismic waves).

However, since the classic inversion algorithm to obtain elastic constants is based on a least-square fitting technique, it is subject to some limitations. Firstly, it is only applicable to samples with 9 unknown elastic constants, which means they must have higher-than-orthorhombic sample symmetries and must be cut along the principal axes. There have been alternative algorithms proposed to overcome this restriction. For example, Sedlak et al. [20] modified the Ritz-Rayleigh method and successfully fitted all 21 elastic constants of triclinic samples by introducing additional constraints of bulk wave speeds. Bales et al. [21] proposed an approach combining Bayesian modelling and Hamiltonian Monte-Carlo, which demonstrated superior convergence over the classic algorithm and could simplify the experimental procedures. The second limitation is that the classic algorithm requires a regular-shaped sample (a sphere, cylindrical or parallelepiped) for efficiently forward modelling the resonant modes in the iterative inversion process. This could be relaxed to arbitrary-shaped samples by the finite element method, as demonstrated in [22], which could also be employed in conjunction with the aforementioned new inversion algorithms.

It must be emphasized that these are limitations of the classic algorithm itself, NOT of the convolution method or the RUS technique in general. In fact, the advancements discussed above could easily be absorbed by this convolution-RUS texture method and broaden its application, to scenarios that are difficult or impossible for conventional water-bath ultrasonics or other existing texture techniques, e.g. on finished components with complex shapes (engine discs, fan blades, or components arising from additive manufacturing), or at elevated temperatures, thus making it a valuable non-destructive texture evaluation tool in its own right.

Acknowledgments

BL gratefully acknowledge Dr. Christopher M. Kube for helpful discussions. The authors would like to thank the Engineering and Physical Sciences Research Council for funding through the HEXMAT programme (EP/K034332/1). RUS facilities in Cambridge were established through grants from the Natural Environment Research Council (NE/B505738/1, NE/F017081/1). The authors also gratefully acknowledge the financial support provided by FRM II for neutron scattering measurements at the Heinz Maier-Leibnitz Zentrum (MLZ), Garching, Germany.

References

[1] U.F. Kocks, C.N. Tome, H.R. Wenk, Texture and Anisotropy: Preferred Orientations in Polycrystals and Their Effect on Materials Properties, Cambridge university press. 2000.
[2] Y. Wang, J. Huang, Mater. Chem. Phys. 81 (2003) 11–26.
[3] B.E. Warren, X-ray Diffraction, Courier Dover Publications. 1969.
[4] A.J. Schwartz, M. Kumar, B.L. Adams, D.P. Field, Electron Backscatter Diffraction in Materials Science, Springer. 2009.
[5] S.D. Sharples, M. Clark, M.G. Somekh, Opt. Express 14 (2006) 10435–10440.
[6] A. Schreyer, H. Clemens, Neutrons and Synchrotron Radiation in Engineering Materials Science: From Fundamentals to Applications, John Wiley and Sons. 2017.
[7] M. Hirao, K. Aoki, H. Fukuoka, J. Acoust. Soc. Am. 81 (1987) 1434–1440.
[8] R. Thompson, J. Smith, S. Lee, G. Johnson, Metall. Trans. A 20 (1989) 2431–2447.
[9] A. Anderson, R. Thompson, C. Cook, Metall. Mater. Trans. A 30 (1999) 1981–1988.
[10] B. Lan, M.J. Lowe, F.P. Dunne, J. Mech. Phys. Solids 83 (2015) 179–198.
[11] B. Lan, M.J. Lowe, F.P. Dunne, J. Mech. Phys. Solids 83 (2015) 221–242.
[12] B. Lan, T.B. Britton, T.-S. Jun, W. Gan, M. Hofmann, F.P. Dunne, M.J. Lowe, Submitted to Acta Mater. 2018.
[13] K. Foster, S. Fairburn, R. Leisure, S. Kim, D. Balzar, G. Alers, H. Ledbetter, J. Acoust. Soc. Am. 105 (1999) 2663–2668.
[14] D.H. Hurley, S.J. Reese, F. Farzbod, J. App. Phys. 111 (2012) 053527.
[15] H. Bunge, Texture Analysis in Materials Science: Mathematical Methods, Butterworths. 1982.
[16] R.E. McKnight, T. Moxon, A. Buckley, P. Taylor, T. Darling, M. Carpenter, J. Phys. Condens. Matter 20 (2008) 075229.
[17] A. Migliori, J.L. Sarrao, Resonant Ultrasound Spectroscopy: Applications to Physics, Material Measurements, and Nondestructive Evaluation, John Wiley & Sons. 1997.
[18] B. Lan, C. Kube, C.-S. Man, M. Carpenter, W. Gan, M. Hofmann, M. Huang, M.J. Lowe, in preparation. 2018.
[19] H.-G. Brokmeier, W. Gan, C. Randau, M. Völler, J. Rebelo-Kornmeier, Nucl. Instrum. Methods Phys. Res. A 642 (2011) 87–92.
[20] P. Sedlák, H. Seiner, J. Zídek, M. Janovská, M. Landa, Exp. Mech. 54 (2014) 1073–1085.
[21] B. Bales, L. Petzold, B.R. Goodlet, W.C. Lenthe, T.M. Pollock, J. Acoust. Soc. Am. 143 (2018) 71–83.
[22] G. Liu, J. Maynard, J. Acoust. Soc. Am. 131 (3) (2012) 2068–2078.